Harmful Algae 143 (2025) 102808

Contents lists available at ScienceDirect

Harmful Algae

journal homepage: www.elsevier.com/locate/hal

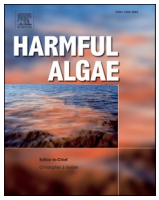

Intraspecific variability within *Karlodinium armiger* (Dinophyceae) on a toxicological and metabolomic level

Magdalena Pöchhacker [a,b,c], Urban Tillmann [d], Doris Marko [b], Elisabeth Varga [a,b,*]

[a] Unit Food Hygiene and Technology, Centre for Food Science and Veterinary Public Health, Clinical Department for Farm Animals and Food System Science, University of Veterinary Medicine, Vienna, Vienna, Austria
[b] Department of Food Chemistry and Toxicology, Faculty of Chemistry, University of Vienna, Vienna, Austria
[c] Doctoral School in Chemistry, Faculty of Chemistry, University of Vienna, Vienna, Austria
[d] Department of Ecological Chemistry, Alfred Wegener Institute Helmholtz Centre for Polar and Marine Research, Bremerhaven, Germany

ARTICLE INFO

Keywords:
Ichthyotoxins
Metabolomics
RTgill-W1
Rhodomonas salina
Karmitoxin

ABSTRACT

The species *Karlodinium armiger* occasionally co-occurs with *Karlodinium veneficum* during harmful algal blooms. The only toxin of this species described so far is karmitoxin, a highly ichthyotoxic compound very similar to the karlotoxins produced by *K. veneficum*. However, information on *K. armiger* is limited and based on a single Mediterranean strain (K-0668), with few studies investigating its toxicity. Given the high intraspecific variability known in *K. veneficum*, it was a significant achievement when two additional strains of *K. armiger* (MD-D6 and MD-D7) were isolated from the Labrador Sea in 2017, enabling comparative studies within this species. The toxicity of these three strains was assessed using the fish gill cell line RTgill-W1 and the cryptophyte *Rhodomonas salina*. An untargeted metabolomics approach using high-resolution tandem mass spectrometry, along with a computational workflow, provided insights into the metabolomic differences between the strains. Despite being cultivated under identical conditions, the metabolomic profiles and toxicological properties were distinct, even between MD-D6 and MD-D7, which were isolated from the same water sample. While MD-D7 did not exhibit significant toxicity, MD-D6 showed high toxicity and lytic potential, similar to K-0668. Interestingly, karmitoxin was only detected in K-0668, and neither karlotoxins nor any known analogs were detected in any strain. Within this comprehensive workflow, some molecules were found in MD-D6 that share the same chemical space as karmitoxin, making them interesting targets for further research. In conclusion, this study evaluated the toxicological and metabolic variability in three different strains of *K. armiger* and identified some putative toxin candidates in MD-D6.

Abbreviations
Karlotoxins (KmTx)
Light microscopy (LM)
Large subunit (LSU)
Internal transcribed spacer (ITS)
Ultra-high-performance liquid chromatography (UHPLC)
High-resolution mass spectrometry (HRMS)
High-resolution mass spectrometry and tandem mass spectrometry (HRMS/MS)
Ethylenediaminetetraacetic acid (EDTA)
CellTiter-Blue® (CTB)
Lactate dehydrogenase (LDH)
Solid-phase extraction (SPE)
Retention time (RT)
Methanol (MeOH)
Quality control (QC)
Formic acid (FA)
Dose-response curve (DRC)
Not available (N.A.)
Principal component analysis (PCA)
Lower limit of detection (LLOD)

* Corresponding author.
E-mail address: elisabeth.varga@vetmeduni.ac.at (E. Varga).

https://doi.org/10.1016/j.hal.2025.102808
Received 27 September 2024; Received in revised form 8 January 2025; Accepted 4 February 2025
Available online 6 February 2025

1. Introduction

Within the genus *Karlodinium* several species are known for their ability to produce bioactive compounds and have been found during harmful algal blooms. *Karlodinium veneficum*, the most extensively studied species within this genus, produces metabolites called karlotoxins (KmTx), a class of amphidinol-like polyketide molecules, described as cytotoxic, ichthyotoxic, and hemolytic (Bachvaroff et al., 2009; Place et al., 2012). There are a few studies implying that structural characteristics are relevant for their mode of action, as these toxins can interact with sterols in the cell membranes of other organisms, forming pores (Deeds and Place, 2006; Place *et al.*, 2009). Fish are particularly susceptible to these toxins, which cause lysis of their gill cells, leading to increased mucus production as a coping mechanism and finally leading to the fish's suffocation (Place *et al.*, 2012).

Karlodinium armiger, first discovered in Alfacs Bay in the Ebro delta in the Mediterranean Sea in 2000, occasionally co-occurs with *K. veneficum* during blooms (Bergholtz *et al.*, 2006; Garcés *et al.*, 2006). The only toxin described so far from *K. armiger* is karmitoxin, a recently identified, highly ichthyotoxic, and lytic compound, which is very similar to KmTx, with a few differences. Notably, the backbone of karmitoxin is longer, with five additional carbon atoms compared to KmTx, and it possesses one primary amine group at the end of its hydrophilic arm (Rasmussen *et al.*, 2017).

While much is known about the toxins and the toxicity of *K. veneficum*, information on *K. armiger* is still limited and is based on a single strain K-0668 from the Mediterranean Sea. Only a few studies have investigated its toxicity in live fish and cell models (Garcés *et al.*, 2006; Fernández-Tejedor *et al.*, 2007; Place *et al.*, 2012; Rasmussen *et al.*, 2017; Binzer et al., 2018, 2020).

In light of the known high intraspecific variability of *K. veneficum* (Calbet *et al.*, 2011), it is a limitation that, until recently, only one strain (the type strain K-0668) of *K. armiger* was available. However, in 2017, we were able to isolate two additional strains (MD-D6 and MD-D7) from the Labrador Sea in the North Atlantic Ocean which opened the route for comparative studies with *K. armiger*. Considering that the environmental conditions of the original location of these two new strains are quite distinct from those of the Mediterranean Ebro Delta, where surface water temperatures can reach up to 28 °C in Alfacs Bay (Cerralbo *et al.*, 2019), compared to 8 °C in the Labrador Sea (Lochte *et al.*, 2020), the question arises if and how this might impact the phenotypes of the strains.

Consequently, the aim of this study was to thoroughly analyze and compare all three strains of *K. armiger* for intraspecific variability in toxicological and metabolic characteristics. For the toxicological assessment, the model fish gill cell line RTgill-W1 and the algal species *Rhodomonas salina* served as valuable alternatives to live fish testing. Additionally, ultra-high-performance liquid chromatography coupled with high-resolution mass spectrometry (UHPLC—HRMS) and tandem mass spectrometry (MS2), combined with an untargeted metabolomics workflow, offered the opportunity to investigate unknown metabolites in all strains.

2. Material and methods

2.1. Strain origin and maintenance

Strain K-0668 of *K. armiger* was previously obtained from the NIVA Culture Collection of Algae (NIVA-CCA). Both strains MD-D6 and MD-D7 were isolated from the Labrador Sea, Station 1 (56°49.42'N; 52°13.15'W) during the MSM65 research cruise of RV Maria S. Merian in the central Labrador Sea in June 2017 by single cell isolation.

The non-axenic stock cultures were maintained at 15 °C and 50–80 µmol photons m^{-2} s^{-1} of cool fluorescent light on a 16:8 hour light:dark cycle. Cells were grown in K-medium (Keller et al., 1987) based on autoclaved seawater collected from the North Sea near Helgoland (salinity of 33). The original K-medium recipe was modified by replacing the organic phosphorus source with 3.62 µM Na_2HPO_4. After addition of the nutrients, the seawater was additionally filter sterilized (0.2 µm).

2.2. Strain characterization

Light microscopy (LM) observation of strain MD-D6 and MD-D7 was performed using living cells with a compound microscope (Axiovert 2; Zeiss, Göttingen, Germany) equipped with epifluorescence and differential interference contrast optics at 1000x magnification. Cells were video-recorded using a digital camera (Gryphax; Jenoptik, Jena, Germany) at full-HD resolution, and single frames were extracted using Corel Video Studio software (Version X8; Corel, Ottawa, ON, Canada).

Cell size of freshly fixed cells (neutral Lugol, 1 % final concentration) from strains during late exponential phase was measured at microscopic magnification of 1000x using the compound microscope and the Axiovision software (Zeiss).

For a molecular characterization of strains MD-D6 and MD-D7, DNA extraction and sequencing of the Internal Transcribed Spacer region (ITS1, 5.8S rRNA, ITS2) and the D1/D2 region of the large subunit (LSU) were conducted using the methods and primers described in Tillmann et al. (2021).

2.3. Cell culture

As a model cell line, RTgill-W1 cells obtained from Kristin Schirmer (Department of Environmental Toxicology, EAWAG, Dübendorf, Switzerland) were used for cytotoxicity tests. This adherent-growing cell line originates from rainbow trout (*Oncorhynchus mykiss*) gills and is a well-established alternative to live fish tests (Organization for Economic Co-operation and Development, 2021). The cultivation of the cells took place in Gibco™ Leibovitz's L-15 medium without phenol red (Thermo Fisher Scientific Inc., Waltham, MA, USA), with 10 % fetal calf serum (Eurobio scientific, Les Ulis, France) and 1 % Gibco™ penicillin-streptomycin (10,000 U/mL) (Thermo Fisher Scientific Inc., Waltham, MA, USA) under sterile and dark conditions, at a temperature of 19 °C. Passaging took place once a week, during which the old cell culture medium was removed, and the cells were washed with Gibco™ Versene solution (Thermo Fisher Scientific Inc., Waltham, MA, USA) prior to trypsinization with 0.25 % trypsin/ 0.02 % ethylenediaminetetraacetic acid (EDTA) in phosphate buffered saline (PBS; PAN Biotech, Aidenbach, Germany). Cells were resuspended in fresh culture medium and centrifuged for 3 min at 50 rcf and 21 °C. After the supernatant was discarded and the cells resuspended in fresh culture medium, 2–2.5 × 10^4 cells cm^{-1} were seeded in T-75 cell culture flasks (Cell+, Sarstedt AG & Co. KG, Nümbrecht, Germany).

2.4. Rhodomonas salina lysis assay

To evaluate extracellular lytic activity, the *K. armiger* strains were grown under the standard culture conditions. At the early stationary growth phase at a cell density of ca. 2.8 × 10^4 cells mL^{-1} as determined by microscopy counts, 30 mL of culture was transferred into 50 mL centrifuge tubes and centrifuged (Eppendorf 5810R, 10 °C, 3220 x g, 10 min). Subsequently, the supernatant was poured into a glass bottle and immediately used for the bioassay. Additionally, subsamples of the supernatant were fixed with Lugol's solution (2 % final concentration) and checked with an inverted microscope to confirm the removal of algal cells. The lytic activity of the supernatants was estimated using the lysis assay described in detail by Tillmann et al. (2009). As the bioassay target species, the cryptophyte *R. salina* (strain KAC 30 from Kalmar culture collection) was used, and this strain was grown under the standard conditions as outlined above.

In brief, triplicate *R. salina* cultures were subjected to varying concentrations of supernatants (equivalent to 1000 to 27,000 cells mL^{-1}) for 24 h including a set of controls (*R. salina* in

K-medium), with a total bioassay volume of 4 mL. After 24 h at 15 °C

in the dark, subsamples were fixed with Lugol's solution (2 % final concentration) and the number of intact *R. salina* cells was determined by inverted microscopic counts.

2.5. Cytotoxicity assays – RTgill-W1

Cytotoxicity assays were conducted in accordance with Schirmer et al. (1997), with modifications as described. RTgill-W1 cells were seeded into 96-well cell culture plates (2×10^4 cells/well; (Cell+, flat base, Sarstedt AG & Co. KG, Nümbrecht, Germany) and incubated for 48 h under sterile and dark conditions at 19 °C. After the incubation time, the cell culture medium was discarded and replaced with the test solutions. *K. armiger* strains (MD-D6, MD-D7 and K-0668) were cultivated in 500 mL Erlenmeyer flasks at the standard culture conditions described in 2.1. until reaching early stationary phase (29,460 cells mL^{-1}, 31,395 cells mL^{-1} and 27,713 cells mL^{-1} respectively). Whole culture samples (including cells) of each strain were shipped in a frozen state to Vienna where they were stored at −20 °C until further analysis took place. For the assessment of their toxic and lytic properties on the fish gill cell line RTgill-W1, 300 µL of thawed whole culture was added to the 96-well plates which were incubated for 3 h in the dark at 19 °C. RTgill-W1 cells incubated with algal K-medium were used as a reference to subtract the impact of the saline conditions in the algal whole culture. Each plate contained at least three technical replicates of each sample, reference, and control. As positive control Triton® X-100 (Carl Roth GmbH + Co. KG, Karlsruhe, Germany) at 0.01 % and 0.005 % was used. For final data evaluation a minimum of two biological RTgill-W1 replicates were generated.

2.5.1. CellTiter-Blue® assay

A CellTiter-Blue® (CTB) assay (Promega Corporation, Fitchburg, MA, USA) was applied to assess the metabolic activity and hence evaluate the viability of RTgill-W1 cells after the incubation with the test substances. CTB reagent contains highly purified and blue colored resazurin, which is reduced within a living cell to the highly fluorescent and pink resorufin. Either absorbance or fluorescence can be measured, but due to higher sensitivity, fluorescence was used (579 nm excitation/584 nm emission). CTB reagent was diluted 1:10 with cell culture medium and conducted according to manufacturer's protocol. After 1 h of incubation in the dark, 80 µL were transferred to a black 96-well ELISA plate (flat base, high binding, Sarstedt AG & Co. KG, Nümbrecht, Germany) and fluorescence was measured using a Biotek® Cytation 3 imaging reader (Agilent Technologies, Inc., Santa Clara, CA, USA).

2.5.2. Lactate dehydrogenase assay

As a second cytotoxicity test, a CyQUANT™ lactate dehydrogenase (LDH) cytotoxicity assay (Thermo Fisher Scientific Inc., Waltham, MA, USA) was used to assess the lytic effect of the test substances on RTgill-W1 cells. This colorimetric assay assesses the release of LDH, a cytosolic enzyme, from the cell to the cell culture medium. If LDH is present, the provided test reagent starts a cascade of enzymatic reactions leading to the red colored product formazan whose absorption can be measured at 490 nm and is proportional to the amount of LDH and thus to cell lysis. The test was conducted as described in the manufacturer's protocol. To be able to perform this test parallel to the CTB assay, 50 µL of the content of each well were transferred to a 96-well ELISA plate (clear, flat base, high binding, Sarstedt AG & Co. KG) without scratching the cell layer on the bottom of the well after the 3 h incubation with whole culture. The amount of cell lysis was calculated in relation to the complete cell lysis achieved with lysis buffer from the test kit. Since it was used for screening of lytic activity, only the three highest concentrations of each strain were tested.

2.6. Untargeted analysis

In addition to cytotoxicity testing, an untargeted metabolomics approach was performed to learn more about the metabolic variances between the three strains.

2.6.1. Solid-phase extraction

Prior to UHPLC—HRMS measurement, solid-phase extraction (SPE) of the thawed whole culture samples, harvested as described in 2.5., was conducted. Since the sample material had a salinity of 33 and interferences in UHPLC—HRMS measurements would probably have occurred, SPE offered the advantage of effectively removing salt from the sample. Strata-X 33 µm Polymeric Reversed Phase cartridges (30 mg, 3 mL, Phenomenex, CA, USA) were conditioned with 2 mL methanol (MeOH), equilibrated with 2 mL water, and loaded with 6 mL thawed whole culture or pure water as a control sample. The cartridges were washed with water, flushed with air until dry, and eluted with 1 mL MeOH directly into a HPLC vial. An aliquot of 300 µL was transferred to a micro insert for immediate analysis, and the rest was stored at −20 °C. All solvents were LC-MS grade quality.

2.6.2. Ultra-high-performance liquid chromatography-high-resolution mass spectrometry

The extracts of MD-D6, MD-D7, K-0668, and a pooled quality control (QC) were then measured using an ultra-high-performance liquid chromatography (UHPLC) (Vanquish, Thermo Scientific, MA, USA) system coupled with a high-resolution mass spectrometer (HRMS) (timsTOF flex, Bruker, MA, USA) with an electrospray ionization source. Separation took place using a Kinetex 1.7 µm F5 100 Å LC column 100 × 2.1 mm (Phenomenex, Aschaffenburg, Germany) at 30 °C with a flow rate of 0.4 mL min^{-1} and 5 µL injection volume. A gradient elution was performed with water as solvent A and acetonitrile/water (90:10, *v/v*) as solvent B, both with 0.1 % formic acid (FA) and all solvents correspond to LC-MS grade quality. At the start, 10 % eluent B was held for 0.5 min, followed by a linear gradient up to 70 % B in 9.5 min, another linear gradient up to 100 % in 2 min, and an isocratic elution for 3 min and back to the initial conditions within 0.5 min, followed by an equilibration time of 3 min before the next run started. The mass spectrometer was operated in positive mode with a capillary voltage of 4.5 kV, a scan range from *m/z* 100 to 2000 and a scan rate of 2 scans per second. The drying gas flow rate was set to 10.0 L min^{-1}, the temperature to 220 °C and the nebulizer pressure was 2.2 bar. Prior to the analysis of samples, the MS was calibrated using an ESI-L Low Concentration Tuning Mix (Agilent Technologies, CA, USA). As acquisition software, otofControl version 6.2 and Compass HyStar 6.0 version 6.0.30.0 (Bruker Daltonics GmbH, MA, USA) were used.

2.6.3. Ultra-high-performance liquid chromatography-high-resolution mass spectrometry and tandem mass spectrometry (UHPLC—HRMS/MS)

To gain further information about the present metabolites in the samples, fragmentation of the features detected in MS1 was necessary. With the information of characteristic MS2 patterns, it was possible to match features with online databases and perform molecular networking to find similarities between different metabolites. MS2 was measured in a follow-up run considering the knowledge about interesting peaks and *m/z* values from the first run. For separation, the same settings were used as before, and the mass spectrometer was operated in positive mode with a capillary voltage of 500 V, a scan range from *m/z* 100 to 2500, and a rate of 4 scans per second. The drying gas flow rate was set to 10.0 L min^{-1}, the temperature to 220 °C, and the nebulizer pressure was 2.2 bar. For fragmentation, auto MS/MS with CID between 20 and 40 was performed with an absolute threshold of 1299 counts and active exclusion after five spectra. Since MS2 spectra have been acquired separately at a later time point, a retention time (RT) shift of approximately 0.25 min was observed. Since the RT was stable within each sequence, this had no impact on the correct evaluation of the data. For better comparison of the results, RT was corrected in some cases.

2.6.4. Metabolomics workflow

To investigate metabolic differences between the three strains of *K. armiger,* a metabolomics approach was used. Therefore, the acquired data were first converted from a vendor-specific to an open file format with the software MSconvert (http://proteowizard.sourceforge.net). Data processing was performed in the statistics software R version 4.2.1 using the packages xcms (Smith et al., 2006; Tautenhahn et al., 2008; Benton *et al.*, 2010), CAMERA (Kuhl et al., 2012) and MSnbase (Gatto and Lilley, 2012; Gatto et al., 2021) and for peak picking the centwave algorithm was selected. According to the visualized chromatogram an intra-peak *m/z* deviation of 10 ppm, an allowed peak width from 3 to 20 s, a minimum of three signals over an intensity threshold of 100, and a minimum signal-to-noise ratio of four was set for peak finding. Peaks with the same RT and *m/z* values were aligned and classified as features, which represented potential metabolites in the sample. To not overlook low-abundant features, gap filling was performed to check for peaks not detected in some samples, due to low intensity but being present in others. Features had to be present in all replicates of one strain; otherwise, they were counted as artefacts and were removed. A water control, treated the same way as whole culture samples, was used for blank subtraction. This step filters all peaks resulting from solvents and possible contaminations during the extraction. By comparing peak shapes and specific mass differences, CAMERA was used to annotate isotopes, fragments, or different adducts to align all features originating from the same metabolite. All detected features were then exported as a csv file, ready for statistical analysis.

All MS2 spectra were analyzed with molecular networking using the online platform GNPS (Wang et al., 2016). Within this analysis, clusters were built based on similar fragmentation patterns to visualize their relationship and the existence of a potential common precursor molecule. Another approach to gain more insight into the molecules present is *in silico* fragmentation, which was performed with the software SIRIUS 5.8.6. Within this method, simulated MS1 and MS2 spectra were generated and compared with the actual experimental data to support the identification of unknown molecules (Dührkop et al., 2019). For data visualization, the software TOPPView version 2.7.0 (Sturm and Kohlbacher, 2009) and Adobe Illustrator version 26.3.1 (Adobe, CA, USA) were used. To evaluate the quality of the formulas proposed by SIRIUS, the isotopic pattern of the most promising candidates was analyzed more closely. Using an isotope pattern calculator (IsoPat v1.11, https://www.researchgate.net/publication/312625688_IsoPat_v111) and isotope cluster spacing (Andersen et al., 2016), the selection of candidates was further refined.

2.7. Statistical analysis

For comparison of the toxic properties in the RTgill-W1 and *Rhodomonas* lysis assay of each strain, a dose-response curve (DRC) was generated and effective concentration (EC_{50}) values, if possible, were calculated, using the package drc (Ritz et al., 2015) in R version 4.2.1. EC_{50}, i.e., the cell density of *K. armiger* corresponding to the concentration of supernatant or whole culture where 50 % of *Rhodomonas* cells were lysed or 50 % viable cells were observed in the CTB assay, was expressed as cells mL^{-1}, including 95 % confidence intervals. The visualization of the DRC was conducted with the package ggplot2 (Wickham, 2016), and statistical significance (p-value < 0.05) was tested with a one-sample *t*-test within R.

Metabolomics data evaluation was carried out with the information from the acquired feature table. Even though gap filling was performed during pre-processing, several zero or "not available" (N.A.) values were present in the feature table, which could lead to difficulties during statistical analysis, for instance in principal component analysis (PCA). To overcome this inflation of zeros, these values were imputed with the lower limit of detection (LLOD), which was determined by selecting the lowest value present in all samples. To get an idea of the quality of the data and to check for cluster formation, the multivariate and unsupervised statistical tool PCA was performed using the R function prcomp, and the scores plot was visualized with the package ggplot2. For univariate analysis data were tested for normal distribution with the Shapiro-Wilk test and homoscedasticity with the Levene test, if the criteria were fulfilled, ANOVA was calculated with the function aov from the R package stats; otherwise, a Kruskal-Wallis test was performed as a non-parametric alternative.

3. Results

3.1. Characterization of the new labrador strains

Both new strains, MD-D6 and MD-D7, were ca. 15–23 µm and 10–20 µm in length and width, respectively (MD-D6: mean length: 18.2 ± 1.6 µm; mean width: 15.6 ± 1.6 µm ($n = 54$); MD-D7: mean length: 19.2 ± 2.1 µm; mean width: 16.4 ± 2.1 µm ($n = 52$). LM analyses of both strains identified the typical cell shape of *Karlodinium* and the presence of a straight acrobase, a ventral pore, several chloroplasts, and a large, elongated nucleus (Fig. 1). Moreover, a BLAST comparison of the newly generated LSU and ITS sequences of both strains MD-D6 (GenBank acc. PQ667057) and MD-D7 (GenBank acc. PQ667058) showed 100 % identity with the respective GenBank entries of the *K. armiger* type strain K-0668, so that both new strains were identified as *K. armiger*.

3.2. Toxicity

3.2.1. RTgill-W1

In the CTB assay, K-0668 ($EC_{50} = 3997$ cells mL^{-1}; 95 % confidence interval 3407 – 4589 cells mL^{-1}) showed the highest impact on cell viability, followed by MD-D6 ($EC_{50} = 7815$ cells mL^{-1}; 95 % confidence interval 7157 – 8473 cells mL^{-1}) (Fig. 2A). MD-D7 showed a non-significant (p-value = 0.065; $t = -3.7$; df = 2) trend at the highest concentration, with high standard deviation. K-0668 and MD-D6 showed lytic activity in the LDH assay, while MD-D7 was not lytic (Fig. 2B).

3.2.2. Rhodomonas salina lysis assay

Cell-free supernatant of both strains K-0668 and MD-D6 caused significant cell lysis of the target species *R. salina* (Fig. 3). In contrast, there was no statistically significant decrease in *R. salina* survival at the highest MD-D7 cell-equivalent densities, thus no lytic activity was observed for this strain (p-value = 0.053; $t = 4.18$; df = 2). For the lytic strains, the EC_{50} value of K-0668 (cell-equivalent density 4600 mL^{-1}; 95 % confidence interval 4300 – 4900) was about 2 times lower (indicating higher lytic activity) compared to strain MD-D6 (cell-equivalent density 9100 mL^{-1}; 95 % confidence interval 8600 – 9700).

3.3. LC—HRMS and LC-HRMS/MS

3.3.1. Presence of karmitoxin

Karmitoxin (*m/z* 1386.89, 6.9 min) and its known analog (*m/z* 1380.84, 6.40 min) were detected in strain K-0668 but not in the strains MD-D6 and MD-D7, neither visually in an extracted ion chromatogram (EIC) (Fig. 4), nor in the automated feature detection using the statistics program R version 4.2.1. Molecular networking did not show any relationship between other molecules and karmitoxin. All samples were also checked for KmTx analogs and KmTx candidates as described in the literature (Place et al., 2012; Krock et al., 2017). None of the karlotoxins described so far were found in any of the samples.

3.3.2. Principal component analysis

PCA presented a cluster formation between the three strains with the highest explained variance on principal component 1 (PC1) of 41.2 % followed by PC2 with an explained variance of 35.7 % (Fig. 5). The number of described features in each strain was approximately 2700, 3200 and 3000 for K-0668, MD-D6 and MD-D7, respectively. In Table S1, the features with the highest variance on PC1 are listed. The

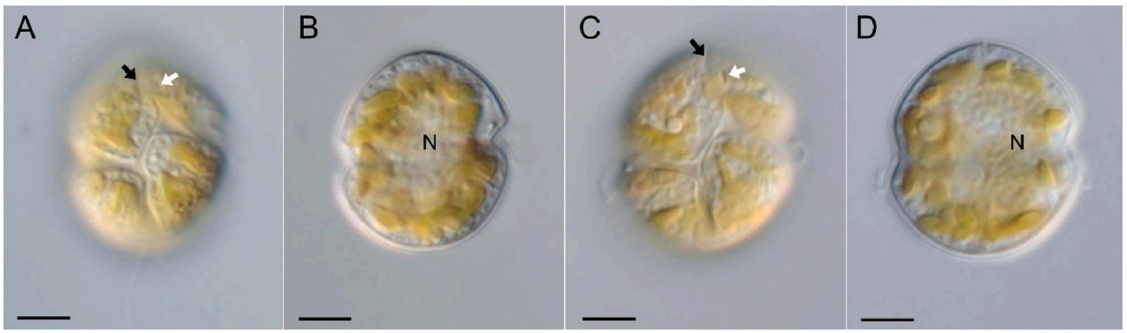

Fig. 1. Light microscopy of the new strains from the Labrador Sea. (A, B) Strain MD-D6. Two focal planes of the same cell. (C, D) Strain MD-D7. Two focal lanes of the same cell. Black arrows: acrobase; white arrows: ventral pore; N = nucleus. Scale bars = 5 µm.

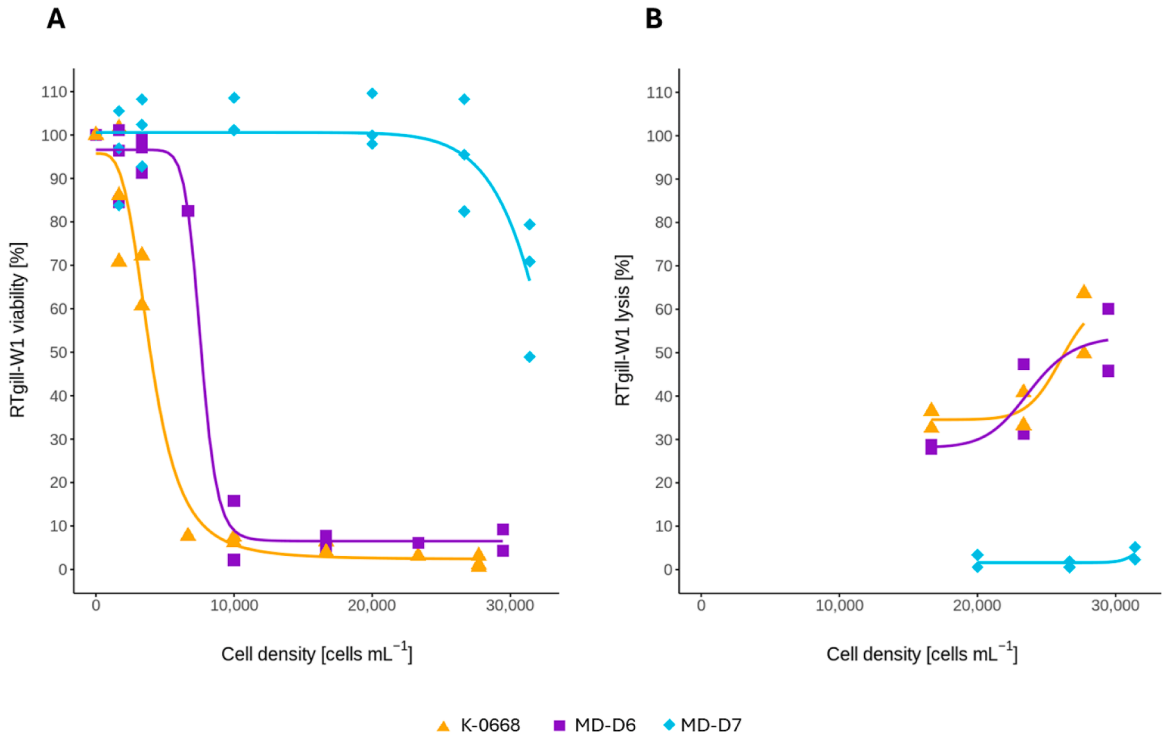

Fig. 2. Toxicity testing on RTgill-W1 cells after 3 h of incubation with thawed whole culture. The x-axis shows the density of the respective algal whole culture. A) CTB assay: RTgill-W1 viability in relation to medium control ($n = 3$). The highest observed toxicity was in K-0668, followed by MD-D6. MD-D7 caused no significant decrease in viability. B) LDH assay: Percentage of cells lysed compared to 100 % lysis of all cells with lysis buffer ($n = 2$). No lytic activity was observed in MD-D7.

features with the highest impact on PC1 are mainly features present only in K-0668. On PC2, a separation of MD-D7 from the other two strains could be observed, and the loadings are provided in Table S2. The highest loadings on PC2 show predominantly features from the end of the chromatographic run, but aside from that, features with high loadings on PC2 are rarely characteristic for MD-D7 but show decreased intensities compared to the other two strains. On PC3 (exp. var. 23.9 %) no separation was seen, except from the QC.

3.3.3. *Molecular networking and in silico fragmentation*

The results of the molecular networking approach provided information about relationships between features found in the samples, as demonstrated for karmitoxin and its analog in K-0668. With this method, further potential analogs, for instance in other strains, can be detected. It was possible to find relationships between features, which seemed to be characteristic for one strain. In a GNPS database query, some compounds were annotated but mainly with a spectral quality of bronze, which does not offer high confidence. These hits, including the score, and the type of classification, (bronze, silver, or gold) (Wang et al., 2016) are listed in the supplements (Table S3). Since most databases are still lacking comprehensive information on MS2 spectra for algal toxins, particular on karlotoxins, *in silico* fragmentation and a database query within SIRIUS were performed in addition to GNPS molecular networking. The combination of both showed some interesting results regarding the potential presence of karmitoxin analogs. In MD-D6, some molecules presented a calculated molecular formula very similar to that of karmitoxin. Since karmitoxin had been assigned the correct molecular formula of $C_{73}H_{127}NO_{23}$ (Rasmussen *et al.*, 2017) in the K-0668 samples by SIRIUS, trust in the system was strengthened. An excerpt of the most promising candidates for karmitoxin/karlotoxin-like molecules in MD-D6 is listed in Table 1 and show besides the detected precursor mass, the potential adducts and calculated molecular formula by SIRIUS with confidence scores. A list with all noteworthy SIRIUS hits can be found in the supplements in Table S4. In Table 1, it is also stated which of these molecules were assigned together in the same molecular network (Fig. 6). The precursor masses in Table 1 were selected due to

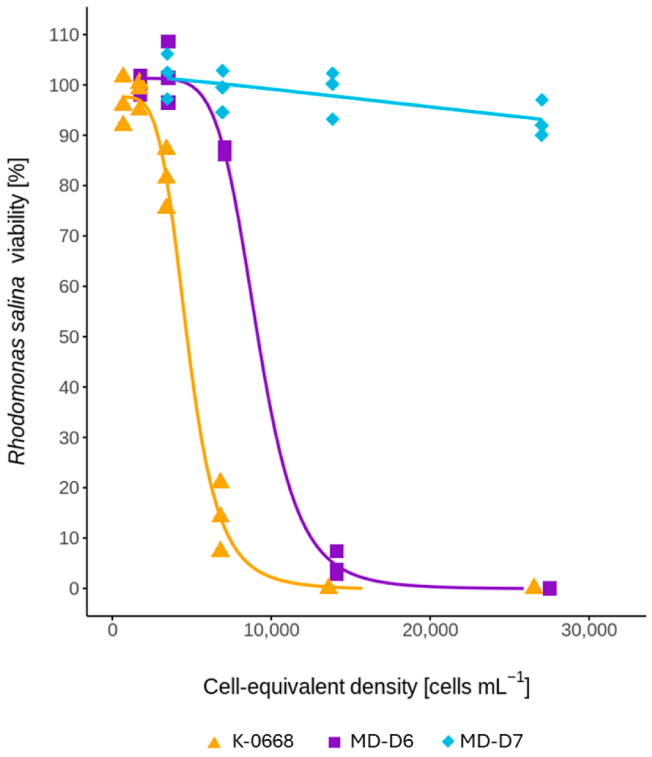

Fig. 3. *Rhodomonas salina* lysis assay: Viability of *R. salina* after incubation with *K. armiger* supernatant for 24 h in comparison to a control ($n = 3$). The x-axis represents the amount of supernatant in the bioassay sample converted into the corresponding cell density of the underlying whole culture at the time point of harvest. The results show that K-0668 had the highest toxic potential, followed by MD-D6, while MD-D7 did not show any significant decrease in *R. salina* survival.

their RT since they formed these prominent feature clusters in Fig. 7, with a similar RT, as karmitoxin. This gives rise to the assumption that most of these features with the same RT are fragments from the same precursor, most likely due to in-source fragmentation. The investigation of the isotopic pattern allowed narrowing down the selection to the described three proposed theoretical molecular formulas. Due to the observed RT shift between MS1 and MS2 measurements, the RT was corrected by 0.25 min to make MS2 and MS1 data more comparable. Sometimes molecular formulas with a lower score are still the preferred option by SIRIUS, which happens if other factors, such as the total explained intensity or explained peaks, contribute to a more trustworthy result.

3.3.4. *Univariate statistics*

Out of 5572 features, 2492 fulfilled the criteria of normal distribution and homoscedasticity and were tested with ANOVA. Of those, 802 features showed significant differences between the three strains with a p-value < 0.05, 482 features with $p < 0.01$, and 246 of these features had a p-value < 0.001.

In total, 3080 features were tested with the non-parametric Kruskal-Wallis test, and 385 features showed significant results with a p-value < 0.05 and no feature had a p-value < 0.01. The results of all statistical tests can be found in Table S5.

4. Discussion

The species *Karlodinium armiger* was first isolated in 2000 by Bergholtz *et al.* (2006) and has been investigated by different research groups since then (Binzer *et al.*, 2018, 2020; Rasmussen *et al.*, 2017; Place et al., 2012; Garcés et al., 2006; Fernández-Tejedor et al., 2007). All insights and discoveries gained during these studies are based on the only available strain, the K-0668, isolated in Alfacs Bay in the Ebro Delta. However, for almost all toxic algal species, there is much evidence for significant intraspecific variability in various traits, including the toxin profile (Miles et al., 2005; Alpermann et al., 2010; Krock *et al.*, 2014; Martens *et al.*, 2017; Binzer et al., 2019). Consequently, information on secondary metabolites is very limited if it is derived from one

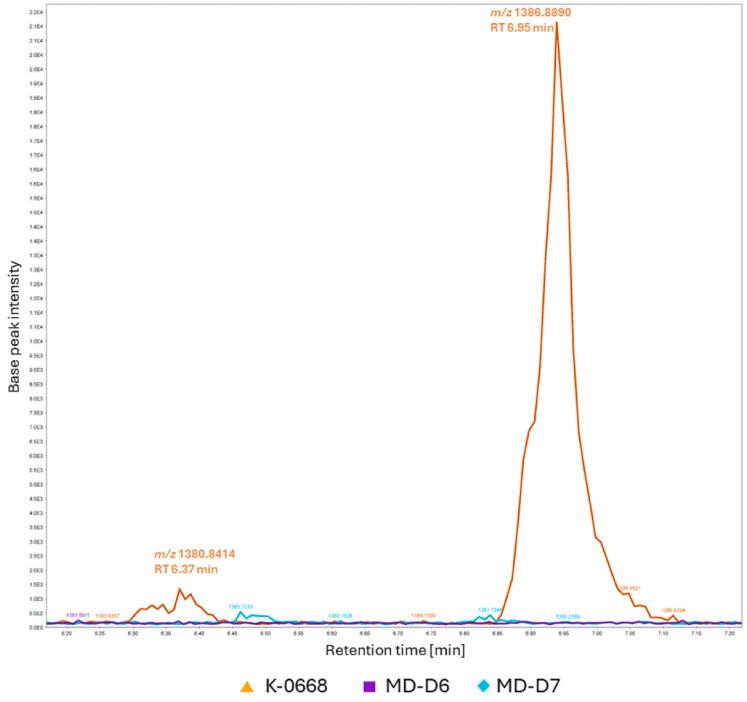

Fig. 4. Extracted ion chromatogram (EIC) of one replicate of each strain, to show the presence of karmitoxin (m/z 1386.8890) and a karmitoxin-analog (m/z 1380.8414) in K-0668 but not in MD-D6 and MD-D7.

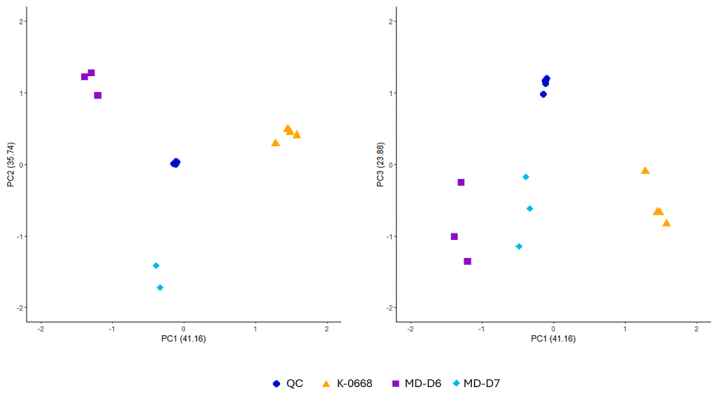

Fig. 5. PCA scores plots: Cluster formation in PC1 and PC2. Highest explained variance on PC1 with 41.16 %. The highest loadings show features that are characteristic of K-0668. No separation of the three strains on PC3 was observed.

Table 1
Potential candidates for karmitoxin/karlotoxin-like molecules in MD-D6. Most promising results from *in silico* fragmentation and molecular networking. The following table presents a theoretical monoisotopic mass with the corresponding molecular formula. The precursor *m/z* represents the mean value ($n = 3$) along with the respective deviation in ppm. The mass error represents the difference between the measured *m/z* and the calculated exact mass. Where applicable, the annotation score is provided for each adduct. A and B indicate the presence of a precursor in a molecular network.

Theoretical monoisotopic mass	Theoretical formula	Precursor (*m/z*)	Mass error (ppm)	Adduct	RT (min) corrected	Zodiac score	Sirius score	Molecular network
1248.7707	$C_{63}H_{112}N_2O_{22}$	1271.7583 (± 1.5 ppm)	1.8	$[M + Na]^+$	6.46	92.3	90.6	B
		1249.7776 (± 2.5 ppm)	0.7	$[M + H]^+$				
		1231.7658 (± 1.5 ppm)	1.7	$[M - H_2O + H]^+$				
		1213.7545 (± 1.5 ppm)	2.4	$[M - 2(H_2O) + H]^+$		49.9	49.6	
973.5318	$C_{53}H_{80}ClNO_{13}$	974.5459 (± 1.5 ppm)	6.4	$[M + H]^+$	6.52	29.0	13.4	A
		956.5378 (± 4.5 ppm)	9.1	$[M - H_2O + H]^+$		96.7	21.9	
		938.5245 (± 3.5 ppm)	6.4	$[M - 2(H_2O) + H]^+$		46.0	15.8	
1282.7258	$C_{70}H_{107}ClN_2O_{17}$	1305.7191 (± 1.5 ppm)	2.7	$[M + Na]^+$	6.83	56.3	66.1	B
		1283.7384 (± 1.5 ppm)	3.7	$[M + H]^+$		92.3	91.5	
		1265.7269 (± 2.0 ppm)	3.0	$[M - H_2O + H]^+$				
		1247.7182 (± 3.5 ppm)	4.6	$[M - 2(H_2O) + H]^+$				

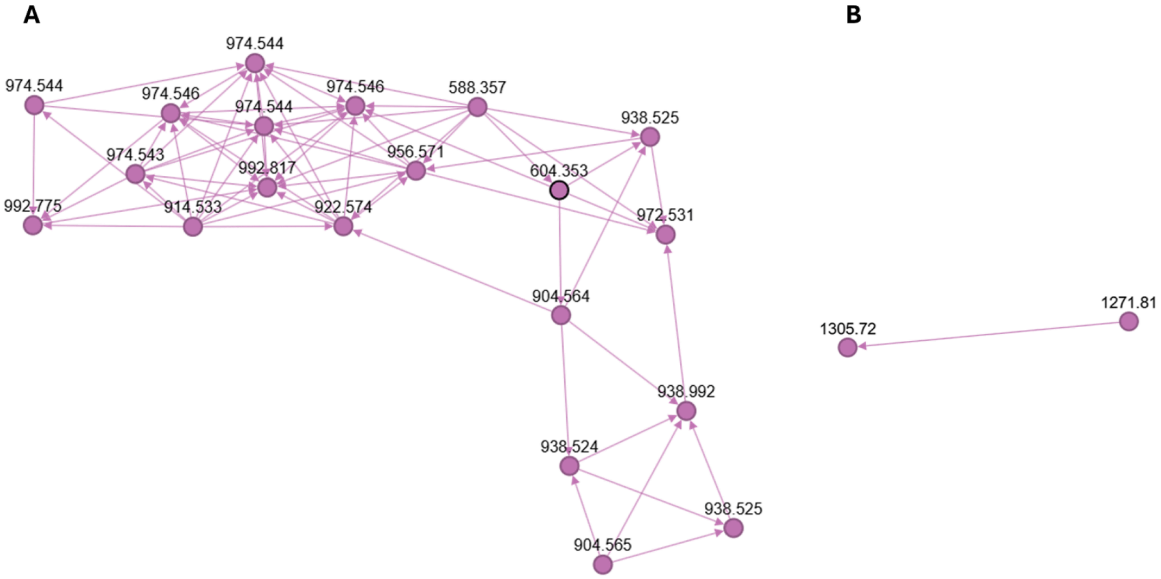

Fig. 6. Two independent molecular networks (A and B) from MS2 data, showing related molecules (nodes = precursor *m/z*) and potential toxin candidates in MD-D6. The distances between the nodes represent the similarity of the molecules based on their spectral pattern.

or very few strains. In relation to *Karlodinium*, Calbet *et al.* (2011) already showed that the intraspecific variability in *K. veneficum* is significant, even between strains derived from the very same bloom. Eleven different strains with identical ITS sequence revealed distinct feeding and growth behavior and metabolic differences, even though they were cultivated under homogenous laboratory conditions. Within the present study, we were able to investigate two more strains of *K. armiger*, isolated from the Labrador Sea. This offered new possibilities and insights

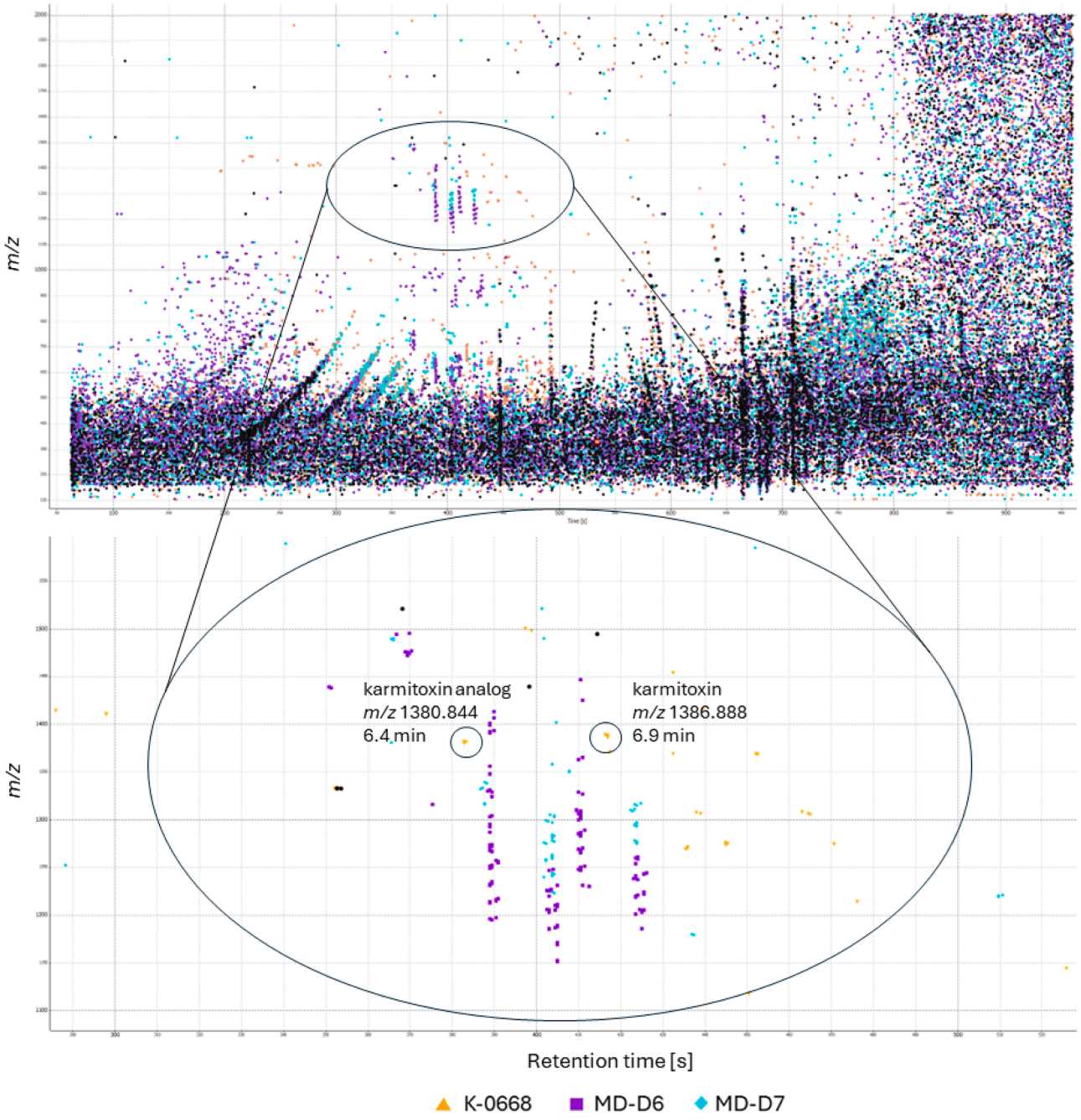

Fig. 7. Total of all detected features (x-axis: RT; y-axis: *m/z*): Black: blank features, which were subtracted for further analysis. Orange triangle: K-0668, purple square: MD-D6 and cyan diamond: MD-D7. The circle represents an area of highly interesting features, which show similar RT and hence similar chemical characteristics to karmitoxin.

into the phenotypical differences, despite the still limited number of strains.

Both LM morphological inspection and the 100 % identity of both LSU and ITS sequence data of MD-D6 and MD-D7 with the type strain K-0668 convincingly showed that all three strains are from the same species. Even though they are identical in their ribosomal marker genes, there are significant differences in secondary metabolite profile and toxicity between these three strains. While MD-D7 did not show significant toxicity and lytic properties in the RTgill-W1 and *Rhodomonas* lysis assays, MD-D6 seemed to be as potent as K-0668 (Fig. 2& 3). Most notably, the only known toxin in *K. armiger* strain K-0668, karmitoxin, was neither present in MD-D6 nor in MD-D7. Due to a lack of analytical standards for karmitoxin and the presence of unknown toxins, at least in MD-D6, the level of toxicity was measured relative to the cell density of the original whole culture, serving as an estimation of their toxic potential. Precautions were taken to make results as comparable as possible between all three strains, which were grown simultaneously, under the same conditions, and harvested at the same growth state and cell density.

One limitation of this study was the use of different sample material for the two cytotoxicity assays. The *Rhodomonas* lysis assay was conducted using the supernatant of the algal cultures, while for RTgill-W1 cytotoxicity assays thawed whole culture, containing biomass, was used. Centrifugation of the thawed whole culture did not alter the results of the assay, as seen in a preliminary experiment. However this discrepancy in sample types could introduce some variables, such as the

impact of biomass or released metabolites from the microalgae during the freeze-thaw process. Despite this potential effect on the comparability of the two tests, the decision to perform it this way, was based on the fact that whole culture was required for the metabolomics experiment and the same sample material was used across these two experimental setups.

Further experiments including HPLC—HRMS/MS revealed new information about all three strains. PCA visualized the metabolic differences with a clear separation between K-0668 and the other two strains on PC1. Moreover, between MD-D6 and MD-D7 a cluster formation was apparent, which was even more pronounced in PC2, where MD-D6 and K-0668 seem to be more related. This gives rise to the question if this separation on PC2 has something to do with the toxicity of the strains. The loadings of PC2 showed that the molecules with the highest impact were present in all three strains, but to a lesser extent in MD-D7, whereas the separation on PC1 was mainly caused by characteristic molecules, only present in K-0668.

Binzer et al. (2020) tested toxicity of purified karmitoxin and whole culture from K-0668 on live sheepshead minnow fish larvae. The results of this study showed that twice the amount of purified karmitoxin was needed compared to the karmitoxin load in the whole culture to achieve the same physical damage. The reason for this outcome remains unclear, but it seems feasible that K-0668 produces other, yet unknown bioactive compounds besides karmitoxin, or that whole culture contains yet undetected toxicity-promoting factors. Assuming that karmitoxin is the leading compound in

K-0668 and responsible for the activity in CTB, LDH, and *Rhodomonas* lysis assays, MD-D6 might produces yet unknown analogs of karmitoxin, KmTx, or other related compounds, since the results resembled those of K-0668 in every conducted assay. Notably, MD-D7 did not show any lytic activity in RTgill-W1 cells and had no significant toxic effect in the CTB or the *Rhodomonas* lysis assay. However, for each CTB assay a slight drop in cell viability was observed for the highest concentration, which had already been observed with undiluted whole culture in previous experiments, with different MD-D7 cultures and cell densities. This was likely an artifact caused by the saline algal medium and unlikely to result from MD-D7′s activity. The sensitivity of RTgill-W1 cells against the highly saline whole cultures was one limitation of this experiment, therefore a second model organism, *R. salina*, which was grown under the same saline conditions, was used to support the results observed in RTgill-W1 assays. In any case, it cannot be excluded that MD-D7 may evoke toxic effects at higher and ecologically unrealistic cell densities. While it is thus not entirely clear whether MD-D7 is capable of producing toxins or not, it is obvious that MD-D6 is, but the question is which ones.

Since online libraries are not very comprehensive for phycotoxins, the database query did not provide sufficient information, but the combination of molecular networking and *in silico* fragmentation offered new insights into potential toxin candidates in MD-D6. With a focus on features only present in MD-D6 with an RT and *m/z* value in the wider range of karmitoxin, i.e., assuming that the unknown toxin has similar properties, some interesting theoretical molecular formulas were suggested by SIRIUS with high confidence scores, which seem to be promising candidates for such a yet unknown karmitoxin-like compound. For some of these candidates, the molecular formula was supported by the results from molecular networking (Table 1) and the use of isotope cluster spacing (Andersen et al., 2016).

In conclusion, based on three *K. armiger* strains, we have shown significant intraspecific variability with respect to metabolic and toxicological profiles. One of the new strains, MD-D6, displayed a very similar toxic and lytic potential to K-0668, without producing the only described toxin so far, karmitoxin, while MD-D7, isolated in the same region as MD-D6, did not have any of these properties. With this very limited number of strains, it was impossible to evaluate whether or to what extent this intra-species variation is driven by contrasting environmental conditions between warm-water Mediterranean and cold-water Labrador Sea populations. Also unknown is the identity of the toxin produced by MD-D6 that caused lysis in RTgill-W1 cells and *R. salina*. Some potential candidates have been selected, which need to be further investigated. There are several approaches that could help with the elucidation of the unknown toxins. Toxicity-guided fractionation is a frequently used tool but requires large-scale algal cultures to produce a sufficient amount of extract for purification. Another possibility would be the derivatization of a terminal amine group, as performed by Andersen et al. (2017) in their indirect quantification method for karmitoxin, in case some of the toxin candidates contain nitrogen, as is the case with karmitoxin. Most importantly, however, the outcome of this study highlights the need for more comprehensive MS databases in the field of algal metabolites, and especially toxins. On the one hand, metabolomic data can identify intraspecific differences and variability among strains, as was done within this and other studies (Hughes et al., 2021). On the other hand, significant chemical differences between strains may coincide with molecular ribotypes, thus supporting a taxonomic differentiation of species, as has been suggested for *Prymnesium parvum* (Binzer et al., 2019). Moreover, single-cell profiling of diatom cultures and field samples revealed some characteristic metabolome features coinciding with the taxonomic identification on the genus level (Baumeister et al., 2020). By contributing to databases by sharing insights into MS raw data and spectra after successful identification, resources could be used more efficiently, and research would be driven forward.

Funding

This research was funded in part by the Austrian Science Fund (FWF) [grant DOI:10.55776/I5707]. For open access purposes, the author has applied a CC BY public copyright license to any author accepted manuscript version arising from this submission. Open access funding was provided by the University of Veterinary Medicine Vienna.

CRediT authorship contribution statement

Magdalena Pöchhacker: Writing – review & editing, Writing – original draft, Visualization, Methodology, Investigation, Formal analysis, Data curation, Conceptualization. **Urban Tillmann:** Writing – review & editing, Writing – original draft, Resources, Methodology, Investigation, Formal analysis, Data curation, Conceptualization. **Doris Marko:** Writing – review & editing, Supervision, Resources, Funding acquisition. **Elisabeth Varga:** Writing – review & editing, Supervision, Resources, Project administration, Methodology, Funding acquisition, Conceptualization.

Declaration of competing interest

The authors declare the following financial interests/personal relationships which may be considered as potential competing interests:

Elisabeth Varga reports financial support was provided by Austrian Science Fund. Urban Tillmann is a member of the Editorial Advisory Board of Harmful Algae. If there are other authors, they declare that they have no known competing financial interests or personal relationships that could have appeared to influence the work reported in this paper.

Acknowledgements

The RTgill-W1 cell line was obtained from Kristin Schirmer, Department of Environmental Toxicology, EAWAG. Furthermore, the authors are grateful to the Mass Spectrometry Centre (MSC), member of the VLSI, Faculty of Chemistry, University of Vienna for technical assistance. Grateful thanks to Hélène-Christine Prause for her valuable input in proofreading and constructive discussions.

Supplementary materials

Supplementary material associated with this article can be found, in the online version, at doi:10.1016/j.hal.2025.102808.

Data availability

We have shared the link to the repository in the manuscript.

References

Alpermann, T.J., Tillmann, U., Beszteri, B., Cembella, A.D., John, U., 2010. Phenotypic variation and genotypic diversity in a planktonic population of the toxigenic marine dinoflagellate *Alexandrium tamarense* (Dinophyceae). J. Phycol. 46 (1), 18–32. https://doi.org/10.1111/j.1529-8817.2009.00767.x.

Andersen, A.J.C., De Medeiros, L.S., Binzer, S.B., Rasmussen, S.A., Hansen, P.J., Nielsen, K.F., Jørgensen, K., Larsen, T.O., 2017. HPLC-HRMS Quantification of the Ichthyotoxin Karmitoxin from *Karlodinium armiger*. Mar. Drugs 15, 278. https://doi.org/10.3390/md15090278.

Andersen, A.J.C., Hansen, P.J., Jørgensen, K., Nielsen, K.F., 2016. Dynamic cluster analysis: an unbiased method for identifying A + 2 element containing compounds in liquid chromatographic high-resolution time-of-flight mass spectrometric data. Anal. Chem. 88 (24), 12461–12469. https://doi.org/10.1021/acs.analchem.6b03902.

Bachvaroff, T.R., Adolf, J.E., Place, A.R., 2009. Strain variation in *Karlodinium veneficum* (Dinophyceae): toxin profiles, pigments, and growth characteristics. J. Phycol. 45 (1), 137–153. https://doi.org/10.1111/j.1529-8817.2008.00629.x.

Baumeister, T.U.H., Vallet, M., Kaftan, F., et al., 2020. Identification to species level of live single microalgal cells from plankton samples with matrix-free laser/desorption ionization mass spectrometry. Metabolomics 16, 28. https://doi.org/10.1007/s11306-020-1646-7.

Benton, H.P., Want, E.J., Ebbels, T.M.D., 2010. Correction of mass calibration gaps in liquid chromatography-mass spectrometry metabolomics data. Bioinformatics 26 (19), 2488–2489. https://doi.org/10.1093/bioinformatics/btq441.

Bergholtz, T., Daugbjerg, N., Moestrup, Ø., Fernández-Tejedor, M., 2006. On the identity of *Karlodinium veneficum* and description of *Karlodinium armiger* sp. nov. (Dinophyceae), based on light and electron microscopy, nuclear-encoded LSU rDNA, and pigment composition. J. Phycol. 42 (1), 170–193. https://doi.org/10.1111/j.1529-8817.2006.00172.x.

Binzer, S.B., Lundgreen, R.B.C., Berge, T., Hansen, P.J., Vismann, B., 2018. The blue mussel *Mytilus edulis* is vulnerable to the toxic dinoflagellate *Karlodinium armiger* - adult filtration is inhibited and several life stages killed. PLoS One 13 (6), e0199306. https://doi.org/10.1371/journal.pone.0199306.

Binzer, S.B., Svenssen, D.K., Daugbjerg, N., Alves-de-Souza, C., Pinto, E., Hansen, P.J., Larsen, T.O., Varga, E., 2019. A-, B- and C-type prymnesins are clade specific compounds and chemotaxonomic markers in *Prymnesium parvum*. Harmf. Algae 81, 10–17. https://doi.org/10.1016/j.hal.2018.11.010.

Binzer, S.B., Varga, E., Andersen, A.J.C., Svenssen, D.K., de, Medeiros LS, Rasmussen, S. A., et al., 2020. Karmitoxin production by *Karlodinium armiger* and the effects of *K. armiger* and karmitoxin towards fish. Harmf. Algae 99, 101905. https://doi.org/10.1016/j.hal.2020.101905.

Calbet, A., Bertos, M., Fuentes-Grünewald, C., Alacid, E., Figueroa, R., Renom, B., Garcès, E., 2011. Intraspecific variability in *Karlodinium veneficum*: growth rates, mixotrophy, and lipid composition. Harmf. Algae 10 (6), 654–667. https://doi.org/10.1016/j.hal.2011.05.001.

F.-Pedrera Balsells M Cerralbo, P., Mestres, M., Fernandez, M., Espino, M., Grifoll, M., et al., 2019. Use of a hydrodynamic model for the management of water renovation in a coastal system. Ocean Sci. 15 (2), 215–226. https://doi.org/10.5194/os-15-215-2019.

Deeds, J.R., Place, A.R., 2006. Sterol-specific membrane interactions with the toxins from *Karlodinium micrum* (Dinophyceae) - a strategy for self-protection? Afr. J. Mar. Sci. 28 (2), 421–425. https://doi.org/10.2989/18142320609504190.

Dührkop, K., Fleischauer, M., Ludwig, M., Aksenov, A.A., Melnik, A.V., Meusel, M., et al., 2019. SIRIUS 4: a rapid tool for turning tandem mass spectra into metabolite structure information. Nat. Methods 16, 299–302. https://doi.org/10.1038/s41592-019-0344-8.

Fernández-Tejedor, M., Soubrier-Pedreño, M.A., Furones, M.D., 2007. Mitigation of lethal effects of *Karlodinium veneficum* and *K. armiger* on *Sparus aurata*: changes in haematocrit and plasma osmolality. Dis. Aquat. Org. 77, 53–59. https://doi.org/10.3354/dao01816.

Garcés, E., Fernandez, M., Penna, A., van Lenning, K., Gutierrez, A., Camp, J., et al., 2006. Characterization of NW mediterranean *Karlodinium* spp. (Dinophyceae) Strains using morphological, molecular, chemical, and physiological methodologies. J. Phycol. 42 (5), 1096–1112. https://doi.org/10.1111/j.1529-8817.2006.00270.x.

Gatto, L., Gibb, S., MSnbase, Rainer J., 2021. Efficient and elegant R-based processing and visualization of raw mass spectrometry data. J. Proteome Res. 20 (1), 1063–1069. https://doi.org/10.1021/acs.jproteome.0c00313.

Gatto, L., Lilley, K.S., 2012. MSnbase-an R/bioconductor package for isobaric tagged mass spectrometry data visualization, processing and quantitation. Bioinformatics 28 (2), 288–289. https://doi.org/10.1093/bioinformatics/btr645.

Hughes, A.H., Florent Magot, F., Tawfike, A.F., et al., 2021. Exploring the chemical space of macro- and micro-algae using comparative metabolomics. Microorganisms 9 (2), 311. https://doi.org/10.3390/microorganisms9020311.

Krock, B., Tillmann, U., Witt, M., Gu, H., 2014. Azaspiracid variability of *Azadinium poporum* (Dinophyceae) from the China Sea. Harmf. Algae 36, 22–28. https://doi.org/10.1016/j.hal.2014.04.012.

Krock, B., Busch, J.A., Tillmann, U., García-Camacho, F., Sánchez-Mirón, A., Gallardo-Rodríguez, J.J., et al., 2017. LC-MS/MS detection of karlotoxins reveals new variants in strains of the marine dinoflagellate *Karlodinium veneficum* from the Ebro Delta (NW Mediterranean). Mar. Drugs 15 (12), 391. https://doi.org/10.3390/md15120391.

Keller, M.D., Selvin, R.C., Claus, R., Guillard, R.R.L., 1987. Media for the culture of oceanic ultraphytoplankton. J. Phycol. 23 (4), 633–638. https://doi.org/10.1111/j.1529-8817.1987.tb04217.x.

Kuhl, C., Tautenhahn, R., Böttcher, C., Larson, T.R., Neumann, S., 2012. CAMERA: an integrated strategy for compound spectra extraction and annotation of liquid chromatography/mass spectrometry data sets. Anal. Chem. 84 (1), 283–289. https://doi.org/10.1021/ac202450g.

Lochte, A.A., Schneider, R., Kienast, M., Repschläger, J., Blanz, T., Garbe-Schönberg, D., et al., 2020. Surface and subsurface Labrador Shelf water mass conditions during the last 6000 years. Climat. Past 16 (4), 1127–1143. https://doi.org/10.5194/cp-16-1127-2020.

Martens, H., Tillmann, U., Harju, K., Dell'Aversano, C., Tartaglione, L., Krock, B., 2017. Toxin variability estimations of 68 *Alexandrium ostenfeldii* (Dinophyceae) strains from The Netherlands reveal a novel abundant gymnodimine. Microorganisms 5 (2), 29. https://doi.org/10.3390/microorganisms5020029.

Miles, C.O., Samdal, I.A., Aasen, J.A.G., Jensen, D.J., Quilliam, M.A., Petersen, D., et al., 2005. Evidence for numerous analogs of yessotoxin in *Protoceratium reticulatum*. Harmf. Algae 4 (6), 1075–1091. https://doi.org/10.1016/j.hal.2005.03.005.

Organization for Economic Co-operation and Development, 2021. Test No. 249: Fish Cell Line Acute Toxicity - The RTgill-W1 Cell Line Assay. OECD. https://doi.org/10.1787/c66d5190-en.

Place, A.R., Bai, X., Kim, S., Sengco, M.R., Wayne Coats, D, 2009. Dinoflagellate host-parasite sterol profiles dictate karlotoxin. J. Phycol. 45 (2), 375–385. https://doi.org/10.1111/j.1529-8817.2009.00649.x.

Place, A.R., Bowers, H.A., Bachvaroff, T.R., Adolf, J.E., Deeds, J.R., Sheng, J., 2012. *Karlodinium veneficum*—the little dinoflagellate with a big bite. Harmf. Algae 14, 179–195. https://doi.org/10.1016/j.hal.2011.10.021.

Rasmussen, S.A., Binzer, S.B., Hoeck, C., Meier, S., de, Medeiros LS, Andersen, N.G., et al., 2017. Karmitoxin: an amine-containing polyhydroxy-polyene toxin from the marine dinoflagellate *Karlodinium armiger*. J. Nat. Prod. 80 (5), 1287–1293. https://doi.org/10.1021/acs.jnatprod.6b00860.

Ritz, C., Baty, F., Streibig, J.C., Gerhard, D, 2015. Dose-response analysis using R. PLoS One 10 (12), e0146021. https://doi.org/10.1371/journal.pone.0146021.

Schirmer, K., Chan, A.G.J., Greenberg, B.M., Dixon, D.G., Bols, N.C., 1997. Methodology for demonstrating and measuring the photocytotoxicity of fluoranthene to fish cells in culture. Toxicol. Vitro 11 (1–2), 107–113. https://doi.org/10.1016/S0887-2333(97)00002-7, 115-9.

Smith, C.A., Want, E.J., O'Maille, G., Abagyan, R., Siuzdak, G, 2006. XCMS: processing mass spectrometry data for metabolite profiling using nonlinear peak alignment, matching, and identification. Anal. Chem. 78 (3), 779–787. https://doi.org/10.1021/ac051437y.

Sturm, M., Kohlbacher, O., 2009. TOPPView: an open-source viewer for mass spectrometry data. J. Proteome Res. 8 (7), 3760–3763. https://doi.org/10.1021/pr900171m.

Tautenhahn, R., Böttcher, C., Neumann, S., 2008. Highly sensitive feature detection for high resolution LC/MS. BMC Bioinform. 9, 504. https://doi.org/10.1186/1471-2105-9-504.

Tillmann, U., Alpermann, T., Da Purificação, R.C., Krock, B., Cembella, A, 2009. Intra-population clonal variability in allelochemical potency of the toxigenic dinoflagellate *Alexandrium tamarense*. Harmf. Algae 8 (5), 759–769. https://doi.org/10.1016/j.hal.2009.03.005, 2009.

Tillmann, U., Wietkamp, S., Gu, H., Krock, B., Salas, R., Clarke, D., 2021. Multiple new strains of *Amphidomataceae* (Dinophyceae) from the North Atlantic revealed a high toxin profile variability of *Azadinium spinosum* and a new non-toxigenic *Az.* cf. *spinosum*. Microorganisms 9 (1), 134. https://doi.org/10.3390/microorganisms9010134.

Wang, M., Carver, J.J., Phelan, V.V., Sanchez, L.M., Garg, N., Peng, Y., et al., 2016. Sharing and community curation of mass spectrometry data with Global Natural Products Social Molecular Networking. Nat. Biotechnol. 34 (8), 828–837. https://doi.org/10.1038/nbt.3597.

Wickham, H., 2016. ggplot2: Elegant Graphics For Data Analysis. 2nd ed. Cham: Springer-Verlag New York. https://doi.org/10.1007/978-3-319-24277-4. Online-Ressource.